DOI: 10.1002/chem.201002105

Induction-Driven Stabilization of the Anion–π Interaction in Electron-Rich Aromatics as the Key to Fluoride Inclusion in Imidazolium-Cage Receptors

Zhaochao Xu,[a, b, d] N. Jiten Singh,[c, d] Sook Kyung Kim,[a] David R. Spring,*[b] Kwang S. Kim,*[c] and Juyoung Yoon*[a]

Abstract: Intermolecular interactions that involve aromatic rings are key processes in both chemical and biological recognition. It is common knowledge that the existence of anion–π interactions between anions and electron-deficient (π-acidic) aromatics indicates that electron-rich (π-basic) aromatics are expected to be repulsive to anions due to their electron-donating character. Here we report the first concrete theoretical and experimental evidence of the anion–π interaction between electron-rich alkylbenzene rings and a fluoride ion in CH_3CN. The cyclophane cavity bridged with three naphthoimidazolium groups selectively complexes a fluoride ion by means of a combination of anion–π interactions and $(C-H)^+\cdots F^-$-type ionic hydrogen bonds. ^1H NMR, ^{19}F NMR, and fluorescence spectra of **1** and **2** with fluoride ions are examined to show that only **2** can host a fluoride ion in the cavity between two alkylbenzene rings to form a sandwich complex. In addition, the cage compounds can serve as highly selective and ratiometric fluorescent sensors for a fluoride ion. With the addition of 1 equiv of F^-, a strongly increased fluorescence emission centered at 385 nm appears at the expense of the fluorescence emission of **2** centered at 474 nm. Finally, isothermal titration calorimetry (ITC) experiments were performed to obtain the binding constants of the compounds **1** and **2** with F^- as well as Gibbs free energy. The **2**-F^- complex is more stable than the **1**-F^- complex by 1.87 kcal mol^{-1}, which is attributable to the stronger anion–π interaction between F^- and triethylbenzene.

Keywords: anions · electron-rich aromatics · fluorides · hydrogen bonds · pi interactions

Introduction

Anion–π interactions have become an actively investigated branch of supramolecular chemistry in recent years.[1–5] Schneider first used the term 'anion–π interaction,' which has pioneered this new field.[6] The study of anion–π interactions gained the momentum to grow as a new research field with the initial ab initio studies of Frontera, Deyà et al.,[7] Mascal et al.,[8] and Alkorta et al.[9] These theoretical studies[7–12] have in turn greatly expedited experiments to provide evidence of anion–π interactions obtained in the solid state[13–19] and in solution[20–23] accompanied by the application of anion–π interactions in anion recognition and binding processes.[24–29]

Anion–π interactions have primarily been studied with electron-deficient aromatics of positive quadrupole moment, such as hexafluorobenzene, 1,3,5-trinitrobenzene, and 1,3,5-triazine, because anion–π interactions that involve electron-rich aromatics with a negative quadrupole moment have generally been expected to be repulsive due to their electron-donating character.[7–12] The noncovalent force between an anion and an electron-deficient aromatic ring has been

[a] Dr. Z. Xu, Dr. S. K. Kim, Prof. J. Yoon
Department of Chemistry and Nanoscience
and Department of Bioinspired Science (WCU)
Ewha Womans University, Seoul, 120-750 (Korea)
Fax: (+82) 232772384
E-mail: jyoon@ewha.ac.kr

[b] Dr. Z. Xu, Dr. D. R. Spring
Department of Chemistry, University of Cambridge
Cambridge, CB2 1EW (UK)
Fax: (+44) 1223336362
E-mail: spring@ch.cam.ac.uk

[c] Dr. N. J. Singh, Prof. K. S. Kim
Center for Superfunctional Materials, Department of Chemistry
Pohang University of Science and Technology (China)
Fax: (+82) 542798137
E-mail: kim@postech.ac.kr

[d] Dr. Z. Xu, Dr. N. J. Singh
Contributed equally to this work.

Supporting information for this article is available on the WWW under http://dx.doi.org/10.1002/chem.201002105.

mainly explained as a contribution of electrostatic attraction between the anion and one of the positive ends of the aromatic quadrupole moment. On the other hand, it is interesting to note that Clements and Lewis theoretically reported that trichlorobenzene/triiodobenzene with negative quadrupole moments can have anion–π interactions.[30] Nevertheless, these compounds are still considered to be an electron-deficient or non-electron-rich system, for which the electrostatic interaction with F^- can be attractive. It is theoretically natural to conclude that electron-rich alkylbenzenes that have negative quadrupole moments would have repulsive anion–π interactions (compound **1**). To substantiate it, we have studied an alkylbenzene with donating substituents (compound **2**). However, surprisingly, we have found that an attractive anion–π interaction does exist for such systems despite the common theoretical knowledge. It is worth mentioning here that Schneider had reported the interaction between a sulfate group and a benzene ring in a 4-[(4-sulfonatophenyl)methyl]benzenesulfonate and *N*-phenylaniline complex.[5,6] The speculation of the anion–π interaction in this system was, however, based solely on the binding free energy without X-ray/NMR spectroscopic structural information. Therefore, given that numerous data of anion–π interactions are available for electron-deficient π systems, it is desirable to have a solid example to provide both clear theoretical understanding and concrete experimental evidence of the anion–π interaction for an electron-rich π system based on well-characterized structures. Here, we report the first theoretical and experimental structural evidence of the anion–π interaction in solution between an electron-rich alkylbenzene ring and a fluoride ion. Furthermore, the anion–π interactions, along with ionic hydrogen bonds, make compound **2** a highly selective host for a fluoride ion.

Results and Discussion

Design and synthesis: Recently, Ballester et al. employed an "enforced proximity" approach in calix[4]pyrrole that derivatives bore axially substituted aryl groups on each of the four *meso* carbon atoms to detect weak chloride–π interactions in solution.[31] Among the various approaches to the recognition of anions,[32,33] the imidazolium group can make a strong interaction with anions through $(C-H)^+\cdots X^-$-type ionic hydrogen bonds in which the charge–charge electrostatic interaction dominates.[34,35] The naphthoimidazolium compound **3** (Scheme 1) was reported as a ratiometric fluorescent chemosensor for a fluoride ion through the strong $(C-H)^+\cdots F^-$-type ionic hydrogen bond, which resulted in a blueshift in emission.[36] As shown in Scheme 1, the extremely rigid cage compounds **1** and **2** contain three imidazolium groups inserted between two substituted benzene rings. The three imidazolium C^2 hydrogen atoms (H^1, C^2–H) in **1** and **2** are directed toward the cyclophane cavity and are shielded by magnetically anisotropic benzene rings that display an unusual chemical shift at high field.[37] However, through an "enforced proximity" approach, only in compound **2** can the

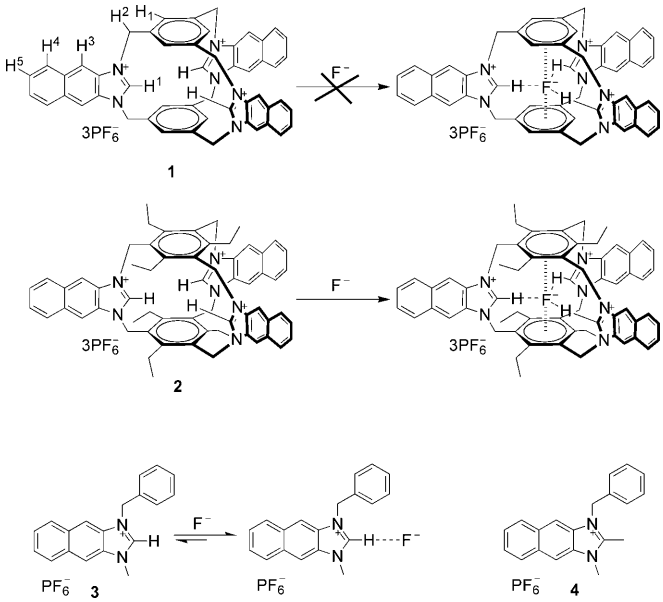

Scheme 1. Structures of compounds **1**–**4**.

three $(C-H)^+\cdots F^-$-type ionic hydrogen bonds position the fluoride ion in the cavity and between these two alkylbenzene rings to form a sandwich complex. The nonrepulsive anion–π interaction between the two electron-rich alkylbenzene rings and the fluoride ion in CD_3CN and DMSO was deduced by ^{19}F and ^1H NMR spectroscopy as well as theoretical calculations. Compound **4** was prepared as a reference.

Reaction of 1*H*-naphtho[2,3-*d*]imidazole (**5**) with 1,3,5-tribromomethylbenzene derivatives **6** and **8** proceeded smoothly to give the 1,3,5-tris[(1*H*-naphtho[2,3-*d*]imidazol-1-yl)methyl]benzene derivatives **7** and **9**, respectively. Cyclophanes **1** and **2** are easily synthesized in good yield by the reaction of 1,3,5-tribromomethylbenzene derivatives with appropriate 1,3,5-tris[(1*H*-naphtho[2,3-*d*]imidazol-1-yl)methyl]benzene derivatives. For example, without recourse to the use of high-dilution conditions, the triply bridged cyclophane **2** was obtained in a good yield of 71% by treatment of 1,3,5-tris(bromomethyl)-2,4,6-triethylbenzene (**8**) with 1,1′,1″-(2,4,6-triethylbenzene-1,3,5-triyl)tris(methylene)tris-(1*H*-naphtho[2,3-*d*]imidazole) (**9**; 1 equiv) in acetone (Scheme 2).[37,38] Compound **1** was synthesized by an analogous route and obtained in 52% yield.

Computational: High-level ab initio coupled-cluster with single and double and perturbative triple/complete basis set (CCSD(T)/CBS)[39] results show that the interaction energies of F^- with benzene (Bz) and triethylbenzene (Et_3Bz) are 0.7 and -0.9 kcal mol^{-1}, respectively (Table 1). Energy component analysis using symmetry-adapted perturbation theory (SAPT)[40,41] reveals that the Bz–F^- and Et_3Bz–F^- complexes have large negative quadrupole moments, and their electrostatic energies ($\approx+6$ kcal mol^{-1}) and exchange energies ($+4$ and 6 kcal mol^{-1}, respectively) are repulsive in

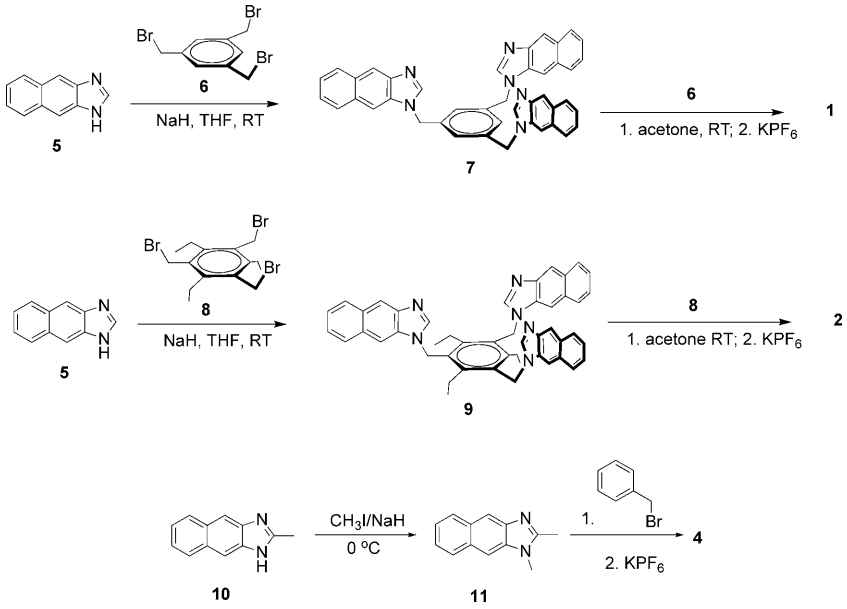

Scheme 2. Synthesis of compounds **1**, **2**, and **4**.

Table 1. Interaction energies (ΔE in kcal mol^{-1}) and distance from F^- to the aromatic ring centroid (d in Å) of various benzene (Bz) derivatives at the level of ab initio and density functional theories.[a]

Complex	$Bz{-}F^-$ [$Bz_2{-}F^-$]	$Et_3Bz{-}F^-$ [$(Et_3Bz)_2{-}F^-$]
Q (HF/6-311G**)[b]	−8.8	−9.1
d (RIMP2/aVDZ)	3.27 [3.11]	3.08 [2.87]
d (TPSS/aVDZ)	3.11 [3.00]	2.95 [2.85]
ΔE(CCSD(T)/CBS)[c]	0.7 [0.6]	−0.9 [−3.2]
ΔE(TPSS)/aVDZ)	0.7 [1.5]	−1.0 [−1.9]
SAPT(MP2)/aVDZ′[d]		
$E_{electrostatic}$	5.7	6.2
$E_{induction**}$[e]	−7.1	−11.1
$E_{dispersion**}$[e]	−1.6	−2.1
$E_{exchange*}$[e]	3.7	6.1

[a] Geometries are optimized at the RIMP2/aug-cc-PVDZ(aVDZ) and DFT-D (TPSS-D/aVDZ) levels. See the Supporting Information for details of the calculations. [b] Quadrupole moments (Q, DÅ) of the uncomplexed aromatic compounds. [c] Calculated at the RIMP2/aVDZ basis set superposition error-corrected geometries. [d] Details of the SAPT results are in the Supporting Information. [e] Asterix is defined in the Supporting Information.

nature. Meanwhile, the dispersion energies (≈ −2 kcal mol^{-1}) are weakly attractive. The repulsive energy terms are mostly compensated by the large attractive induction energy term (−7 and −11 kcal mol^{-1}, respectively). Therefore, although the $Bz{-}F^-$ complex is not yet stabilized, the $Et_3Bz{-}F^-$ complex is stabilized. Hence, despite the large negative quadrupole moment (≈ −9 DÅ), the highly polarizable Et_3Bz binds F^- with their strong anion-induced polarization by F^-. This type of interaction is quite different from that of the F^- complexes with positive quadrupole moments due to electron-deficient rings.

As the second π system is added to a complex in which the π system interacts with F^- (i.e., as the $Et_3Bz{-}F^-$ complex changes to the $(Et_3Bz)_2{-}F^-$ complex), the latter sandwiched system is highly stabilized with a greatly enhanced interaction energy (−4.3 kcal mol^{-1}; cf. −1.5 kcal mol^{-1} of the 1:1 complex) and a greatly shortened distance (d) between F^- and the aromatic ring centroid (2.87 Å, which is reduced from 3.08 Å). This is because the higher excess electron density migration from F^- to two π rings due to higher polarization dramatically stabilizes the 2:1 complex relative to the 1:1 complex. In the case of the Bz-F^--Bz complex, the F^- ion is still in a repulsive potential; thus, this sandwiched complex is not stabilized. We also observed a similar trend in the calculated geometrical and energetic results using density functional theory with empirical dispersion corrections (DFT-D (TPSS-D/aVDZ)),[42] even though the anion-induced polarization effect is weaker. Hence, the utilization of Et_3Bz as the tripodal base of a cage structure allows accommodation of an F^- anion inside the cage, whereas such accommodation of a F^- anion is not possible in the case of benzene as a tripodal base. With this theoretical understanding, we proceeded to check if F^- can be captured inside the cage of the rigid framework of compound **2**.

Experimental evidence: The ^1H and ^{19}F NMR spectra as well as fluorescence properties of **1** and **2** with fluoride ions were examined to verify the inclusion of fluoride in the cavity. As reference data, the NMR spectra and fluorescence properties of **3** with F^- were reported previously.[35] The $(C{-}H)^+{\cdots}F^-$ interaction blueshifts the fluorescence of **3** from 440 to 372 nm. The chemical shifts of $C^2{-}H$ and F^- change from $\delta = 9.08$ to 9.52 ppm and from $\delta = -115.4$ (free F^- in CD_3CN) to −150.9 ppm, respectively. However, the electrostatic interaction between the imidazolium cation and F^- can only quench the fluorescence without a shift in emission, which is supported by the titration test with **4** (Figure S1 in the Supporting Information). This indicates the key role of $C^2{-}H$ in the interaction with fluoride. Therefore, the δ of $C^2{-}H$ and the blueshift in the fluorescence emission can be used to probe the hydrogen bond between $C^2{-}H$ and F^-.

^1H NMR spectra of **1** and **2** upon the addition of fluoride are shown in Figure 1. Tetrabutylammonium fluoride hydrate was used as the fluoride source. With the addition of fluoride, the peaks of $C^2{-}H$ (H^1) in **1** shifted downfield slightly from $\delta = 6.82$ to 7.30 ppm (Figure 1b). However, for **2**, upon fluoride binding, the singlet peak of $C^2{-}H$ (H^1) substantially shifted downfield ($\delta = 6.43$ to 12.60–12.81 ppm for **2** in Figure 1e) and split into a doublet ($J = 84$ Hz, spin–spin

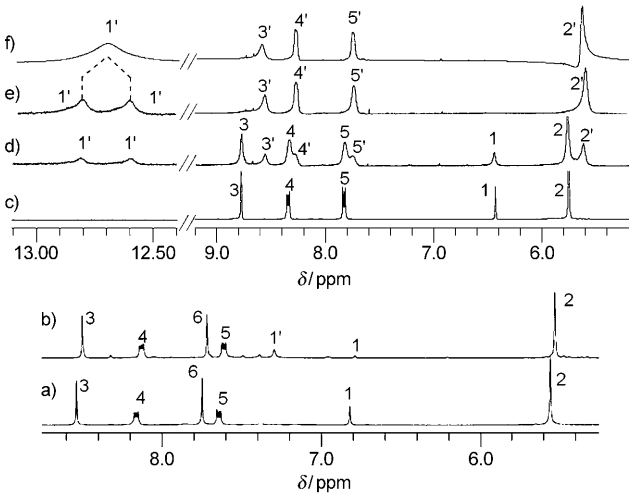

Figure 1. ^{1}H NMR spectra of **1** and **2** with fluoride in CD_3CN at room temperature. a) Compound **1** with 0 equiv of F^-; b) **1** with 1.0 equiv of F^-; c) **2** with 0 equiv of F^-; d) **2** with 0.5 equiv of F^-; e) **2** with 1 equiv of F^-, ^{19}F coupled; f) **2** with 1 equiv of F^-, ^{19}F decoupled. [**2**] = 7.5 mM.

coupling between C^2–H and F^-), whereas the resonances of H^2,H^5 significantly shifted upfield. The ^{1}H NMR spectra of **2**-F^- with fluorine decoupling display the δ of C^2–H as a broad singlet at $\delta = 12.71$ ppm.

The fluorescence responses of **1** and **2** to various anions were then examined. As shown in Figure 2a, with the addition of 1 equiv of F^-, a strongly increased fluorescent emission centered at 385 nm appeared at the expense of the fluorescent emission of **2** centered at 474 nm. Other tested anions quenched the fluorescence without a shift in emission; the extent of quenching depends on the nature of the anion. However, the addition of fluoride quenched the fluorescence of **1** with the electrostatic interaction between the imidazolium and fluoride anion (Figure 2b). These results support the selective inclusion of F^- in the cavity of **2** through $(C–H)^+\cdots F^-$ ionic hydrogen bonds. The fluorescence titration experiment of **2** with F^- showed the dependence of the ratio of the emission intensities at 375 and 474 nm (I_{375}/I_{474}) on the concentration of F^- (Figure 2c). Thus, **2** could also be used for ratiometric fluorescent probing for F^- (see the Supporting Information for details), which means that changes in the ratio of the emission intensities at two wavelengths are observed.

^{19}F NMR spectroscopy was carried out to explore the F^-–π interaction in solution. The resonances of PF_6^- appear as a doublet between $\delta = -70$ and -73 ppm. Upon the inclusion of fluoride in the cavity of **2**, as shown in Figure 3a, the singlet peak of free F^- was substantially shifted upfield ($\delta = -115.4$ to

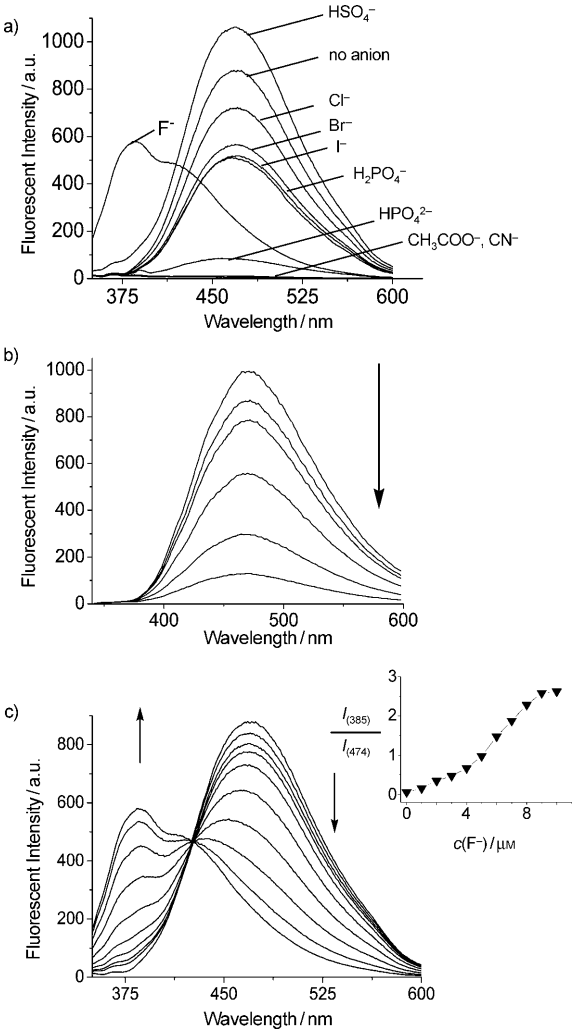

Figure 2. a) Fluorescence responses of **2** (10 μM) to various anions (1 equiv). b) Fluorescence spectra of **1** (10 μM) in the presence of different concentrations of F^- (0 to 1 equiv) in CH_3CN. c) Fluorescence spectra of **2** (10 μM) in the presence of different concentrations of F^- (0 to 1 equiv) in CH_3CN. Inset: Ratiometric calibration curve I_{385}/I_{474} as a function of the F^- concentration.

−47.01–47.66 ppm due to the strong interaction between F^- and the two benzene rings) and split into a quartet (J = 84 Hz, spin–spin coupling between C^2–H and F^-). The cou-

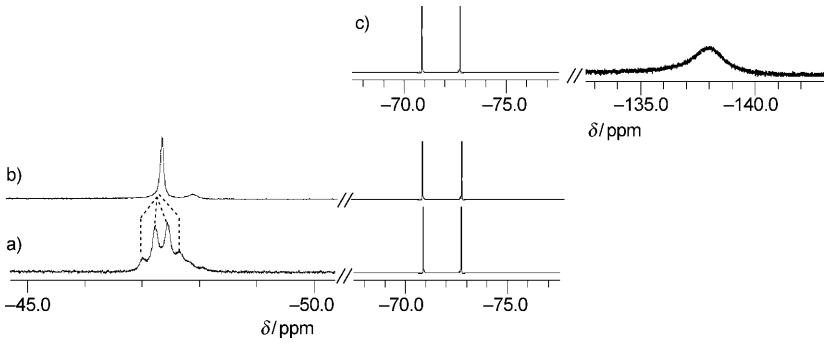

Figure 3. ^{19}F NMR spectra of **1** and **2** with 1 equiv of fluoride in CD_3CN at room temperature. a) Compound **2**, ^{1}H coupled; b) **2**, ^{1}H decoupled. [**2**] = 7.5 mM; c) **1**.

pling constant is the same as that of C^2–H in Figure 1e. The ^{19}F spectrum of **2**-F^- with proton decoupling displays the chemical shift of F^- at $\delta = -47.34$ ppm as a sharp singlet (Figure 3b). The quartet shown in Figure 3a is consistent with the hypothesis that F^- is in the center of the cavity and interacts equally with the three C^2–H groups. However, in the mixture of **1**-F^- (1:1), the singlet peak of free F^- is shifted downfield from $\delta = -115.4$ to -138.05 ppm due to the electrostatic interaction (Figure 3c). Further studies indicate that F^- can also interact with only two or one C^2–H in the cavity of **2** to form a benzene–F^-–benzene sandwich complex and to display the F^-–π interaction, which may depend on the concentration of the **2**-F^-complex. For example, when the concentration of **2**-F^- is lower than 6.2 mM, the triplet and doublet peaks for two and one $(C–H)^+\cdots F^-$ ionic hydrogen bonds, respectively, are observed in the ^{19}F NMR spectra. Correspondingly, two groups of doublet peaks appear in the ^1H NMR spectra. Moreover, the ^{19}F,^1H HOESY spectrum also confirms the strong contact between F^- and C^2–H nuclei (see the Supporting Information). This reflects the stepwise polarization induced by F^- during the course of F^- capture from the outside to the center of the cavity. After a period of time, the lower concentration sample displayed the same NMR spectroscopic signals with the higher concentration sample, indicating that the F^- is in the center of the cavity and interacts equally with the three $(C–H)^+$ groups.

To check the effect of solvent on the anion–π interaction, the binding properties of **1** and **2** with F^- in DMSO were investigated through ^1H and ^{19}F NMR spectroscopy as well as fluorescence spectra. The upfield-shifted F^- at $\delta = -49.20$ ppm indicates the existence of an F^-–π interaction in DMSO for compound **2** (see the Supporting Information). Correspondingly, the singlet peak of C^2–H (H^1) shifted downfield and split into a doublet (spin–spin coupling between C^2–H and F^-), whereas the resonances of H^2,H^5 significantly shifted upfield (see the Supporting Information). However, a broad singlet at about $\delta = -157.5$ ppm in the ^{19}F NMR spectra was also observed, which was mostly due to the C^2–F bond formation. Then the addition of F^- into DMSO quenched the fluorescence of **2** with a slight blue-shift in emission (see the Supporting Information).

Isothermal titration calorimetry (ITC) experiments: The binding constants of compounds **1** and **2** with F^- were obtained by means of isothermal titration calorimetry (ITC) experiments at 25 °C (Table 2). The ITC plots show that the stoichiometry of **1**-F^- is 1:2, whereas **2** binds F^- in a 1:1 pattern. This also provides evidence that F^- only approaches imidazolium molecules outside the cavity of **1**, whereas F^- is hosted in the cavity of **2** to interact with three imidazolium molecules equally. In the case of **1**, the first F^- could be bound with two imidazolium moieties and the second F^- with the third imidazolium moiety. Since triply charged imidazolium host systems and F^- anions are solvated very effectively (as acetonitrile molecules around the hosts are strongly polarized and well ordered), the positive ΔH value at room temperature indicates the endothermic reorganization of the solvent shells into a less-ordered form upon host–F^- complex formation. This is due to the fact that the reduced charge of the host–F^- complex by ion pairing results in the substantial reduction of the dipole-charge interaction with the less-ordered solvent. The complex is less solvated than the sum of its free components (verified by the formation of precipitation in ^1H NMR spectroscopic titration in which the higher concentration of host was used in the ITC experiment); thus, the release of solvent molecules to the bulk leads to the entropic overcompensation of the unfavorable positive ΔH of desolvation.[43,44]

Table 2. Isothermal titration calorimetry (ITC)-determined binding constants ($\times 10^4\,M^{-1}$) and thermodynamic quantities [kcal mol^{-1}] for (**1**–**2**)-F^- complexes. Theoretically estimated free energies are in square brackets.

	Compound **1**	Compound **2**
n	1.89 ($\approx$2)[a]	1.07[a]
K_a	6.62 (K_1), 0.0335 (K_2)[b]	68.0
ΔG	−6.07 (ΔG^1) [−5.59] −2.41 (ΔG^2) [−1.02]	−7.94 [−7.91]
ΔH	2.93 (ΔH^1), 16.36 (ΔH^2)	3.86
$T\Delta S$	9.00 (ΔS^1), 18.77 (ΔS^2)	11.80

[a] "One set of sites" binding model. [b] "Sequential binding sites" model, **1**/F = 1:2.

Molecular modeling: Furthermore, we have investigated the structural isomers and energetics of the **1**-F^- and **2**-F^- complexes using DFT-D (TPSS-D/aVDZ)[41,42] with the consideration of solvent treatment using the conductor-like screening model (COSMO).[45] The optimized geometries of **1**-F^- and **2**-F^- complexes show that the isomers with the F^- ion outside/inside (external/internal isomers) the cage of **1**/**2** are thermodynamically more favorable (Figure 4). The estimated binding free energies[34] of the **1**-F^- ($-\Delta G^1$, $-\Delta G^2$) and **2**-F^- complexes are respectively 5.58 kcal mol^{-1} for 1:1 binding mode, 1.02 kcal mol^{-1} for 1:2 binding mode, and 7.91 kcal mol^{-1}, which are in good agreement with the ITC

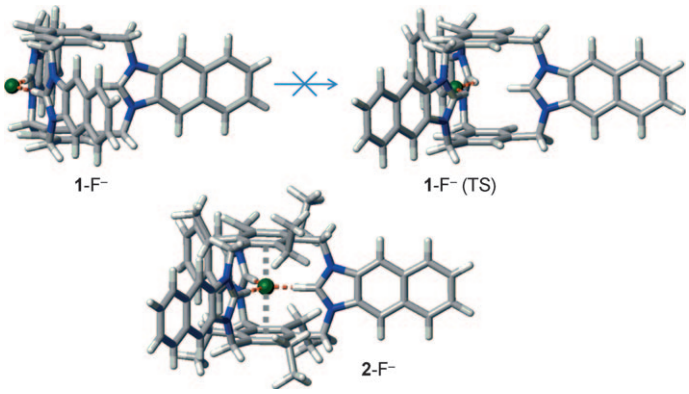

Figure 4. Thermodynamically favorable optimized structures of complexes **1**-F^- (external isomer) and **2**-F^- (internal isomers) at the TPSS-D/aVDZ level of theory in acetonitrile solvent. The transition-state structure (TS) **1**-F^- is approximately 10.5 kcal mol^{-1} higher than that of **1**-F^- external structure, yet around 5.6 kcal mol^{-1} higher than that of **2**-F^-.

experimental values of 6.07, 2.41, and 7.94 kcal mol^{-1} (Table 2). The relative free-energy stabilization of the **2**-F$^-$ complex with respect to the **1**-F$^-$ complex from the ITC data is 1.9 kcal mol^{-1}; the theoretical data gives 2.3 kcal mol^{-1}. Additionally, the transition-energy barrier relative to the most stable isomer of the **1**-F$^-$ and **2**-F$^-$ complexes with F$^-$ outside the cage toward the formation of structures with F$^-$ inside the cage were calculated to be around 10.5 and 5.6 kcal mol^{-1}, respectively. Therefore, at the experimental temperature (25 °C), the external isomer of the **1**-F$^-$ complex with two strong (C–H)$^+$···F$^-$ ionic hydrogen bonds could cross the transition-energy barrier of 10.5 kcal mol^{-1} to form the internal isomer (calculated to be equally stable as that of the external isomer due to enhanced interaction from the imidazolium moieties); however, this internal structure would be thermodynamically unfavorable due to the unfavorable anion–π interaction. On the contrary, in the case of the **2**-F$^-$ complex, as the external isomer is approximately 6 kcal mol^{-1} less stable than the internal isomer, the formation of the latter isomer would be easily feasible by crossing the transition-energy barrier of approximately 6 kcal mol^{-1}. Therefore, F$^-$ is stabilized inside the cage of **2** with the formation of (C–H)$^+$···F$^-$ ionic hydrogen bonds, whereas the anion–π interaction, though small, is key for the selectivity of F$^-$.

Conclusion

In summary, by using highly accurate ab initio calculations of electron-rich aromatic model systems, we predict for the first time that anion–π interactions are possible even for electron-rich aromatic systems when the induction effect is large enough to compensate for the electrostatic repulsion. Such anion–π interactions have been demonstrated by experimentally verifying the inclusion of fluoride in the rigid framework of trisimidazolium cage **2** in which electron-rich triethylbenzene is a tripodal base. The unique inclusion pattern of fluoride with the formation of (C–H)$^+$···F$^-$ ionic hydrogen bonds and the anion–π interaction between the electron-rich alkylbenzene and fluoride has been demonstrated with fluorescent changes, ^{19}F and ^{1}H NMR spectroscopic titrations, and theoretical calculations.

Experimental Section

Materials and methods: Unless otherwise noted, materials were obtained from commercial suppliers and were used without further purification. Flash chromatography was carried out on silica gel 60 (230–400 mesh ASTM; Merck). Thin-layer chromatography (TLC) was carried out using Merck 60 F_{254} plates with a thickness of 0.25 mm. Preparative TLC was performed using Merck 60 F_{254} plates with a thickness of 1 mm. ^{1}H, ^{13}C, and ^{19}F NMR spectra were recorded using a Bruker instrument operating at 250 or 400 MHz. Chemical shifts (δ) were given in ppm and coupling constants (J) in Hz. Fluorescence emission spectra were obtained using an RF-5301/PC spectrofluorophotometer from Shimadzu.

Synthesis of compound 7: NaH (300 mg, 7.5 mmol, 60% in mineral oil) was added at 0 °C to a reaction mixture of **5**[46] (300 mg, 1.8 mmol) in THF (20 mL). After the reaction mixture was stirred for 20 min at 0 °C, **6** (210 mg, 0.59 mmol) was added. After additional stirring for 1 h at room temperature, the reaction mixture was added to water (50 mL) and was extracted with $CHCl_3$. The organic layer was then separated, dried with anhydrous sodium sulfate, and concentrated under reduced pressure. Purification by flash chromatography on silica gel (CH_2Cl_2/MeOH = 100:1) afforded **7** as a white solid (247 mg, 68%). ^{1}H NMR ($CDCl_3$, 400 MHz): δ = 5.26 (s, 6H), 6.95 (s, 3H), 7.33–7.42 (m, 9H), 7.55 (d, J = 8.0 Hz, 3H), 7.98 (d, J = 8.0 Hz, 3H), 8.06 (s, 3H), 8.27 ppm (s, 3H); ^{13}C NMR ($CDCl_3$, 62.5 MHz): δ = 48.28, 105.54, 117.83, 123.80, 124.81, 125.12, 127.39, 128.20, 128.55, 130.18, 130.55, 134.00, 137.98, 143.81, 146.86 ppm; HRMS (FAB): m/z: calcd for $C_{42}H_{31}N_6$: 619.2610 [M+H$^+$]; found: 619.2602.

Synthesis of compound 1: Acetone (20 mL) was added to a mixture of **6** (0.087 g, 0.24 mmol) and **7** (0.15 g, 0.24 mmol). The mixture was stirred at room temperature for 20 h. The precipitate was filtered to give **1**-Br_3 as white solid. The bromide salt was dissolved in DMF (10 mL). During the dropwise addition of saturated aqueous KPF_6 solution, a precipitate was formed. After washing the precipitate several times with water, the desired product was obtained as a light yellow solid (146 mg, 52%). ^{1}H NMR (CD_3CN, 250 MHz): δ = 5.56 (s, 12H), 6.82 (s, 3H), 7.65 (dd, 6H), 7.75 (s, 6H), 8.16 (dd, 6H), 8.54 ppm (s, 6H); ^{13}C NMR (CD_3CN, 100 MHz): δ = 51.12, 111.87, 112.54, 128.52, 131.85, 132.84, 135.76, 136.06, 143.44 ppm; HRMS (FAB): m/z: calcd for $C_{51}H_{39}F_{12}N_6P_2$: 1025.2520 [M–PF$_6$]$^+$; found: 1025.2512.

Synthesis of compound 9: NaH (300 mg, 7.5 mmol, 60% in mineral oil) was added at 0 °C to a reaction mixture of **5** (300 mg, 1.8 mmol) in THF (20 mL). After the reaction mixture was stirred for 20 min at 0 °C, compound **8**[47] (250 mg, 0.57 mmol) was added. After additional stirring for 1 h at room temperature, the reaction mixture was added to water (50 mL) and extracted with $CHCl_3$. The organic layer was then separated, dried over anhydrous sodium sulfate, and concentrated under reduced pressure. Purification by flash chromatography on silica gel (CH_2Cl_2/MeOH = 100:1) afforded **9** (327 mg, 82%) as a white solid. ^{1}H NMR ($CDCl_3$, 250 MHz) δ = 0.85 (t, J = 6.6 Hz, 9H), 2.60 (m, 6H), 5.32 (s, 6H), 7.34 (m, 6H), 7.53 (s, 3H), 7.75 (s, 3H), 8.87 (t, J = 8.0 Hz, 6H), 8.22 ppm (s, 3H); ^{13}C NMR ($CDCl_3$, 62.5 MHz): δ = 15.58, 23.84, 43.07, 105.23, 117.98, 123.91, 124.98, 127.51, 128.70, 130.23, 130.43, 130.65, 134.57. 143.93, 144.84, 146.54 ppm; HRMS (FAB): m/z: calcd for $C_{48}H_{43}N_6$: 703.3549 [M+H$^+$]; found: 703.3552.

Synthesis of compound 2: Acetone (20 mL) was added to a mixture of **8** (0.075 g, 0.17 mmol) and **9** (0.12 g, 0.17 mmol). The mixture was stirred at room temperature for 20 h. The precipitate was filtered to give **2**-Br_3 as white solid. The filtrate was concentrated to $^1/_3$ volume and the new precipitate was filtered again. The total product was 144 mg in 74% yield. ^{1}H NMR (CD_3OD, 250 MHz): δ = 1.15 (s, 18H), 2.49 (s, 12H), 5.83 (s, 12H), 6.37 (s, 3H), 7.78 (d, 6H), 8.31 (d, 6H), 9.03 ppm (s, 6H); ^{13}C NMR (CD_3OD, 62.5 MHz): δ = 16.42, 24.63, 46.56, 113.23, 128.84, 129.81, 130.56, 132.88, 133.93, 150.65 ppm. The bromide salt was dissolved in methanol (20 mL). During the dropwise addition of saturated aqueous KPF_6 solution, precipitate was formed. After washing the precipitate several times with water, the desired product was obtained as a light yellow solid (93 mg, 71%). ^{1}H NMR (CD_3CN, 250 MHz): δ = 1.32 (s, 18H), 2.48 (s, 12H), 5.76 (s, 12H), 6.43 (s, 3H), 7.82 (d, 6H), 8.34 (d, 6H), 8.79 ppm (s, 6H); ^{13}C NMR (CD_3CN, 62.5 MHz): δ = 14.98, 22.77, 45.15, 112.03, 127.49, 128.20, 128.28, 131.46, 131.75, 136.39, 149.07 ppm; HRMS (FAB): m/z: calcd for $C_{63}H_{63}F_{12}N_6P_2$: 1193.4398 [M–PF$_6$]$^+$; found: 1193.4392.

Synthesis of compound 11: NaH (330 mg, 8.3 mmol, 60% in mineral oil) was added at 0 °C to a reaction mixture of **10**[45] (746 mg, 4.1 mmol) in THF (20 mL). After the reaction mixture was stirred for 20 min at 0 °C, iodomethane (960 mg, 6.3 mmol) was added. After additional stirring for 1 h at room temperature, the reaction mixture was added to water (50 mL) and extracted with $CHCl_3$. The organic layer was then separated, dried over anhydrous magnesium sulfate, and concentrated under reduced pressure. Purification by flash chromatography on silica gel

(CH_2Cl_2/MeOH = 100:1) afforded **11** (740 mg, 92%) as a pale yellow solid. ^{1}H NMR ($CDCl_3$, 250 MHz): δ = 2.64 (s, 3H), 3.73 (s, 3H), 7.25 (m, 1H), 7.40 (m, 2H), 7.60 (m, 1H), 7.93 (m, 2H), 8.13 ppm (m, 1H); ^{13}C NMR ($CDCl_3$, 62.5 MHz): δ = 14.09, 29.62, 104.37, 115.28, 123.21, 123.98, 127.41, 128.31, 129.98, 132.53, 136.45, 142.71, 156.14 ppm; HRMS (FAB): *m*/*z*: calcd for $C_{13}H_{13}N_2$: 197.1079 [M+H$^+$]; found: 197.1082.

Synthesis of compound 4: A mixture of **11** (100 mg, 0.51 mmol) and benzyl bromide (130 mg, 0.76 mmol) in acetonitrile (10 mL) was heated at reflux for 24 h under N_2. After cooling to the room temperature, the precipitate was filtered and washed with cold CH_2Cl_2 to give **4** as bromide salt. The bromide salt was dissolved in methanol (10 mL). During the dropwise addition of aqueous saturated KFP_6 solution, precipitate was formed. After washing the precipitate with water several times, the desired product was obtained as a white solid (165 mg, 75%). ^{1}H NMR (DMSO, 250 MHz): δ = 2.90 (s, 3H), 4.03 (s, 3H), 5.71 (s, 2H), 7.38 (m, 5H), 7.65 (m, 2H), 8.10 (m, 3H), 8.31 ppm (m, 1H); ^{13}C NMR (DMSO, 62.5 MHz): δ = 10.71, 31.57, 48.43, 109.79, 109.86, 117.02, 117.66, 117.79, 126.42, 126.90, 127.79, 127.85, 128.36, 128.80, 129.99, 130.71, 130.94, 131.03, 133.14, 155.74 ppm; HRMS (FAB): *m*/*z*: calcd for $C_{20}H_{19}N_2$: 287.1543 [$M-PF_6$]$^+$; found: 287.1540.

Calculation methods: Interaction energies of benzene–F$^-$ (Bz–F$^-$) and triethylbenzene–F$^-$ (Et_3Bz–F$^-$) complexes are calculated on the optimized geometries at the level of RIMP2/aug-cc-pVDZ (abbreviated as aVDZ) theory with the basis-set superposition-error (BSSE) correction. These optimized geometries were used for the further calculation of RIMP2/aVTZ and CCSD(T)/aVDZ single-point energies with BSSE corrections. The complete basis set (CBS) limit values for the RIMP2 interaction energies were evaluated based on the extrapolation method by exploiting the fact that the basis set error in the electron correlation energy is proportional to N^{-3} for the aug-cc-pV*N*Z (or aV*N*Z) basis set.[39] The CCSD(T)/CBS interaction energies were estimated by calculating the sum of CCSD(T)/aVDZ interaction energies and the difference between the RIMP2/CBS and RIMP2/aVDZ interaction energies. Meanwhile, the CCSD(T)/CBS interaction energies of $(Bz)_2$–F$^-$/$(Et_3Bz)_2$–F$^-$ complexes were estimated as the sum of the MP2/CBS interaction energy and twice the [CCSD(T)/CBS–MP2/CBS] energy for the respective Bz–F$^-$/Et_3Bz–F$^-$ complexes. Additionally, geometry optimization and energy calculations were also performed using density functional theory with empirical dispersion correction at the TPSS-D/aVDZ level, which gives energy values close to the CCSD(T)/CBS limit. This calculation for large systems lends credence to the estimated CCSD(T)/CBS results for the large systems. More details are provided in the Supporting Information. The calculation details of SAPT are in the Supporting Information.

Isothermal titration calorimetry experiments: Isothermal titration calorimetry experiments were performed using a VP-ITC microcalorimeter (Microcal Inc., Northampton, MA). All solutions were prepared in HPLC-grade MeCN. For a typical ITC run, the instrument chamber (1.4 mL) contained a solution of the host ([**1**] = 0.1 mM, [**2**] = 0.1 mM), and a 2.0 mM solution of tetrabutylammonium fluoride (guest) was taken up in a 300 μL injection syringe. The syringe was assembled into the chamber for equilibration while stirring at 502 rpm. The chamber temperature was set up to 25 °C. The injections were programmed at 10 μL each, added over 20 s, and spaced 200 s apart. "Number of sites" (N), binding constant (K in M^{-1}), association enthalpy (ΔH in cal mol^{-1}), and association entropy (ΔS in cal mol^{-1} K^{-1}) were obtained by fitting the titration data using the "one set of sites" model algorithm provided in the MicroCal Origin Software package (version 7.0). For compound **1**, the curve-fitting "sequential binding sites" model was also used.

Acknowledgements

We thank Dr. Nick Bampos for helpful discussions. Y.J. acknowledges financial support from the Basic Science Research Program (2010-0018895), the Converging Research Center Program (2009-0093677), and WCU (R31-2008-000-10010-0) through the National Research Foundation; K.S.K. acknowledges the National Honor Scientist Program, GRL, WCU (R32-2008-000-10180-0), the EPB Center (2009-0063312), KISTI (KSC-2008K08-0002), D.R.S. acknowledges the Herchel Smith Postdoctoral Fellowship Fund and the Newman Trust.

[1] P. Gamez, T. J. Mooibroek, S. J. Teat, J. Reedijk, *Acc. Chem. Res.* **2007**, *40*, 435–444.
[2] B. P. Hay, V. S. Bryantsev, *Chem. Commun.* **2008**, 2417–2428.
[3] B. L. Schottel, H. T. Chifotides, K. R. Dunbar, *Chem. Soc. Rev.* **2008**, *37*, 68–83.
[4] N. J. Singh, H. M. Lee, I.-C. Hwang, K. S. Kim, *Supramol. Chem.* **2007**, *19*, 321–332.
[5] J. L. Sessler, S. Camiolo, P. A. Gale, *Coord. Chem. Rev.* **2003**, *240*, 17–55.
[6] a) H.-J. Schneider, T. Schiestel, P. Zimmermann, *J. Am. Chem. Soc.* **1992**, *114*, 7698–7703; b) H.-J. Schneider, T. Schiestel, P. Zimmermann, *J. Phys. Org. Chem.* **1993**, *6*, 590–594.
[7] D. Quiñonero, C. Garau, C. Rotger, A. Frontera, P. Ballester, A. Costa, P. M. Deyà, *Angew. Chem.* **2002**, *114*, 3539–3542; *Angew. Chem. Int. Ed.* **2002**, *41*, 3389–3392.
[8] M. Mascal, A. Armstrong, M. D. Bartberger, *J. Am. Chem. Soc.* **2002**, *124*, 6274–6276.
[9] I. Alkorta, I. Rozas, J. Elguero, *J. Am. Chem. Soc.* **2002**, *124*, 8593–8598.
[10] C. Garau, A. Frontera, D. Quiñonero, P. Ballester, A. Costa, P. M. Deyà, *ChemPhysChem* **2003**, *4*, 1344–1348.
[11] D. Kim, P. Tarakeshwar, K. S. Kim, *J. Phys. Chem. A* **2004**, *108*, 1250–1258.
[12] D. Y. Kim, N. J. Singh, J. W. Lee, K. S. Kim, *J. Chem. Theory Comput.* **2008**, *4*, 1162–1169.
[13] S. Demeshko, S. Dechert, F. Meyer, *J. Am. Chem. Soc.* **2004**, *126*, 4508–4509.
[14] P. de Hoog, P. Gamez, I. Mutikainen, U. Turpeinen, J. Reedijk, *Angew. Chem.* **2004**, *116*, 5939–5941; *Angew. Chem. Int. Ed.* **2004**, *43*, 5815–5817.
[15] C. S. Campos-Fernández, B. L. Schottel, H. T. Chifotides, J. K. Bera, J. Bacsa, J. M. Koomen, D. H. Russell, K. R. Dunbar, *J. Am. Chem. Soc.* **2005**, *127*, 12909–12923.
[16] I. A. Gural'skiy, P. V. Solntsev, H. Krautscheid, K. V. Domasevitch, *Chem. Commun.* **2006**, 4808–4810.
[17] S. Furukawa, T. Okubo, S. Masaoka, D. Tanaka, H. Chang, S. Kitagawa, *Angew. Chem.* **2005**, *117*, 2760–2764; *Angew. Chem. Int. Ed.* **2005**, *44*, 2700–2704.
[18] C. Estarellas, M. C. Rotger, M. Capó, D. Quiñonero, A. Frontera, A. Costa, P. M. Deyà, *Org. Lett.* **2009**, *11*, 1987–1990.
[19] R. J. Götz, A. Robertazzi, I. Mutikainen, U. Turpeinen, P. Gamez, J. Reedijk, *Chem. Commun.* **2008**, 3384–3386.
[20] H. Maeda, A. Osuka, H. Furuta, *J. Inclusion Phenom. Macrocyclic Chem.* **2004**, *49*, 33–36.
[21] Y. S. Rosokha, S. V. Lindeman, S. V. Rosokha, J. K. Kochi, *Angew. Chem.* **2004**, *116*, 4750–4752; *Angew. Chem. Int. Ed.* **2004**, *43*, 4650–4652.
[22] O. B. Berryman, F. Hof, M. J. Hynes, D. W. A. Johnson, *Chem. Commun.* **2006**, 506–508.
[23] R. M. Fairchild, K. T. Holman, *J. Am. Chem. Soc.* **2005**, *127*, 16364–16365.
[24] V. Gorteau, G. Bollot, J. Mareda, A. Perez-Velasco, S. Matile, *J. Am. Chem. Soc.* **2006**, *128*, 14788–14789.
[25] M. Mascal, I. Yakovlev, E. B. Nikitin, J. C. Fettinger, *Angew. Chem.* **2007**, *119*, 8938–8940; *Angew. Chem. Int. Ed.* **2007**, *46*, 8782–8784.
[26] A. P. Davis, D. N. Sheppard, B. D. Smith, *Chem. Soc. Rev.* **2007**, *36*, 348–357.
[27] L. A. Barrios, G. Aromi, A. Frontera, D. Quinonero, P. M. Deyà, P. Gamez, O. Roubeau, E. J. Shotton, S. J. Teat, *Inorg. Chem.* **2008**, *47*, 5873–5881.
[28] C. Hung, A. S. Singh, C. Chen, Y. Wen, S. Sun, *Chem. Commun.* **2009**, 1511–1513.

[29] R. E. Dawson, A. Hennig, D. P. Weimann, D. Emery, V. Rauikumar, J. Montenegro, T. Takeuchi, S. Gabutti, M. Mayor, J. Mareda, C. A. Schalley, S. Matile, *Nat. Chem.* **2010**, *2*, 533–538.
[30] A. Clements, M. J. Lewis, *J. Phys. Chem. A* **2006**, *110*, 12705–12710.
[31] G. Gil-Ramírez, E. C. Escudero-Adán, J. Bene *t*Buchholz, P. Ballester, *Angew. Chem.* **2008**, 120, 4182–4186; *Angew. Chem. Int. Ed.* **2008**, *47*, 4114–4118.
[32] a) R. Martínez-Máñez, F. Sancanón, *Chem. Rev.* **2003**, *103*, 4419–4476; b) T. Gunnlaugsson, M. Glynn, G. M. Tocci, P. E. Kruger, F. M. Pfeffer, *Coord. Chem. Rev.* **2006**, *250*, 3094–3117; c) C.-H. Lee, H. Miyaji, D.-W. Yoon, J. L. Sessler, *Chem. Commun.* **2008**, 24–34; d) T. Sakamoto, A. Ojida, I. Hamachi, *Chem. Commun.* **2009**, 141–152; e) Z. Xu, X. Chen, H. N. Kim, J. Yoon, *Chem. Soc. Rev.* **2010**, *39*, 127–137; f) C. Caltagirone, P. A. Gale, *Chem. Soc. Rev.* **2009**, *38*, 520–563; g) H. Y. Gong, B. M. Rambo, E. Karnas, V. M. Lynch, J. L. Sessler, *Nat. Chem.* **2010**, *2*, 406–409; h) X. Chen, Y. Zhou, X. Peng, J. Yoon, *Chem. Soc. Rev.* **2010**, *39*, 2120–2135.
[33] a) Y. Kubo, T. Ishida, T. Minami and T. D. James, *Chem. Lett.* **2006**, *35*, 996–997; b) Y. Kubo, A. Kobayashi, T. Ishida, Y. Misawa, T. D. James, *Chem. Commun.* **2005**, 2846–2848; c) Z. Q. Guo, W. H. Zhu, H. Tian, *Macromolecules* **2010**, *43*, 739–774; C. W. Chiu, F. P. Gabbaï, *J. Am. Chem. Soc.* **2006**, *128*, 14248–14249; d) S. K. Kim, J. H. Bok, R. A. Bartsch, J. Y. Lee, J. S. Kim, *Org. Lett.* **2005**, *7*, 4839–4842; e) D. H. Lee, H. Y. Lee, K. H. Lee, J.-I. Hong, *Chem. Commun.* **2001**, 1188–1189; f) J. L. Sessler, W.-S. Cho, V. Lynch, V. Král, *Chem. Eur. J.* **2002**, *8*, 1134–1143; g) S.-J. Hong, J. Yoo, D.-W. Yoon, J. Yoon, J. S. Kim, C.-H. Lee, *Chem. Asian J.* **2010**, *5*, 768–772; h) Q.-Q. Jiang, B. Darhkijav, H. Liu, F. Wang, Z. Li, Y.-B. Jiang, *Chem. Asian J.* **2010**, *5*, 543–549; i) Y. Qu, J. Hua, H. Tian, *Org. Lett.* **2010**, *12*, 3320–3323; j) E. J. Jun, K. M. K. Swamy, H. Bang, S.-J. Kim, J. Yoon, *Tetrahedron Lett.* **2006**, *47*, 3103–3106.
[34] a) J. Yoon, S. K. Kim, N. J. Singh, K. S. Kim, *Chem. Soc. Rev.* **2006**, *35*, 355–360; b) Z. Xu, S. K. Kim, J. Yoon, *Chem. Soc. Rev.* **2010**, *39*, 1457–1466.
[35] a) S. K. Kim, B.-G. Kang, H. S. Koh, Y. J. Yoon, S. J. Jung, B. Jeong, K.-D. Lee, J. Yoon, *Org. Lett.* **2004**, *6*, 4655–4658; b) K. Chellappan, N. J. Singh, I. C. Hwang, J. W. Lee, K. S. Kim, *Angew. Chem.* **2005**, *117*, 2959–2963; *Angew. Chem. Int. Ed.* **2005**, *44*, 2899–2903; c) S. K. Kim, N. J. Singh, J. Kwon, I.-C. Hwang, S. J. Park, K. S. Kim, J. Yoon, *Tetrahedron* **2006**, *62*, 6065–6072; d) V. Amendola, B. Colasson, L. Fabbrizzi, M.-J. R. Douton, *Chem. Eur. J.* **2007**, *13*, 4988–4997; e) C. Coll, R. Casasús, R. Martínez-Máñez, M. D. Marcos, F. Sancenón, J. Soto, *Angew. Chem.* **2007**, *119*, 1705–1708; *Angew. Chem. Int. Ed.* **2007**, *46*, 1675–1678; f) Z. Xu, N. J. Singh, J. Lim, J. Pan, H. N. Kim, S. Park, K. S. Kim, J. Yoon, *J. Am. Chem. Soc.* **2009**, *131*, 15528–15533; g) X. Chen, S. Kang, M. J. Kim, J. Kim, Y. S. Kim, H. Kim, B. Chi, S.-J. Kim, J. Y. Lee, J. Yoon, *Angew. Chem.* **2010**, *122*, 1448–1451; *Angew. Chem. Int. Ed.* **2010**, *49*, 1422–1425.
[36] Z. Xu, S. K. Kim, S. J. Han, G. Kociok-Kohn, T. D. James, J. Yoon, *Eur. J. Org. Chem.* **2009**, 3058–3065.
[37] M. V. Baker, M. J. Bosnich, C. C. Williams, B. W. Skelton, A. H. White, *Aust. J. Chem.* **1999**, *52*, 823–825.
[38] C. E. Willans, K. M. Anderson, P. C. Junk, L. J. Barbour, J. W. Steed, *Chem. Commun.* **2007**, 3634–3636.
[39] S. K. Min, E. C. Lee, H. M. Lee, D. Y. Kim, D. Kim, K. S. Kim, *J. Comput. Chem.* **2008**, *29*, 1208–1221.
[40] B. Jeziorski, R. Moszynski, K. Szalewicz, *Chem. Rev.* **1994**, *94*, 1887–1930.
[41] N. J. Singh, S. K. Min, D. Y. Kim, K. S. Kim, *J. Chem. Theory Comput.* **2009**, *5*, 515–529.
[42] a) J. M. Tao, J. P. Perdew, V. N. Staroverov, G. E. Scuseria, *Phys. Rev. Lett.* **2003**, *91*, 146401; b) S. Grimme, *J. Comput. Chem.* **2006**, *27*, 1787–1799.
[43] M. Berger, F. P. Schmidtchen, *Angew. Chem.* **1998**, *110*, 2840–2842; *Angew. Chem. Int. Ed.* **1998**, *37*, 2694–2696.
[44] M. Haj-Zaroubi, N. W. Mitzel, F. P. Schmidtchen, *Angew. Chem.* **2002**, *114*, 111–114; *Angew. Chem. Int. Ed.* **2002**, *41*, 104–107.
[45] A. Klamt, G. Schüürmann, *J. Chem. Soc. Perkin Trans.2* **1993**, 799–805.
[46] A. Hijazi, W. Pfleiderer, *Nucleosides Nucleotides* **1984**, *3*, 549–557.
[47] A. Vacca, C. Nativi, M. Cacciarini, R. Pergoli, S. Roelens, *J. Am. Chem. Soc.* **2004**, *126*, 16456–16465.

Received: July 23, 2010
Published online: December 13, 2010

